

# Wind effects on roof-mounted solar photovoltaic arrays: CFD and wind-tunnel evaluation

Robert N. Meroney<sup>a</sup> and David E. Neff<sup>b</sup>

<sup>a</sup>Colorado State University, Fort Collins, CO, USA, Robert.Meroney@ColoState.Edu

<sup>b</sup>Colorado State University, Fort Collins, CO, USA, David.Neff@ColoState.Edu

**ABSTRACT:** Numerical calculations of wind loads on solar photovoltaic collectors were used to estimate drag, lift and overturning moments on different collector support systems. These results were compared with direct force measurement tests obtained during wind tunnel experiments. The numerical procedure employed k-epsilon, RNG and k-omega turbulence closures to predict loads. The RNG and k-omega model approaches produced reasonable agreement with measured loads, whereas the k-epsilon model failed to replicate measurements. Numerically generated particle path lines about the model collectors strongly resembled wind-tunnel smoke visualization observations.

## 1 INTRODUCTION

Commercial rooftops are an excellent location for photovoltaic (PV) modules. These roofs provide exposure to abundant sun light, offer a secure and robust place for PV module installation located away from public access, and the panels are located in close proximity to the energy user. Today there are an estimated 11 million square feet of PV modules installed on both flat and sloped rooftops in the United States (O'Brien, 2006). Solar experts working to install arrays on rooftops have found that estimation of wind loads (uplift, side loads and overturning moments) are critical to their satisfactory performance (Barkaszi and Dunlop, 2001; Adrian et al., 1986). Although the UL, IEC, and IEEE standards for PV do not address roof-specific issues, such systems must comply with the National Electric Code (NEC) and local building codes, such as the International Building Code (IBC). Eventually mounting systems may be certified by Factory Mutual (FM) or the International Building Code Council (ICC), and, meanwhile, engineers are attempting to determine wind loads on PV arrays using IBC and ASCE recommendations for minimum design loads on buildings (ASCE 7-05). Unfortunately, the unique configuration of some solar systems suggest that they may experience either higher or lower wind loads than predicted by codes (Healey, 2009). Hence, an alternative approach to determine wind loads using analysis, CFD or laboratory testing is frequently employed ( Lee and Bienkiewicz, 1995; Neff and Bienkiewicz, 2000; Neff and Meroney, 2003).

Ballasted systems are commonly used to secure PV modules to flat roofs. The equipment is kept in place on the flat roof by its own weight as well as careful aerodynamic design. Wind tunnel measurements are frequently employed to measure loads on individual and arrays of ballasted photo collectors, but the number required can become extensive and cumbersome if one desires to consider many alternative configurations. Computational Fluid Dynamics (CFD) can provide a flexible and cost-effective tool to select promising configurations from alternative design strategies, which can be subsequently tested in detail either in the laboratory or the field. This paper reports the results of a series of calculations that created CFD simulations of selected direct force measurements obtained during wind tunnel experiments. These were used to refine computational algorithms and evaluate the use of CFD to predict aerodynamic loading on individual PV tiles within tile arrays. Only static loading produced by a steady horizontal wind was considered for this exercise.

## 2 WIND-TUNNEL MODELING PROGRAM

A five-component ( $F_x$ ,  $F_y$ ,  $F_z$ ,  $M_x$ , and  $M_y$ ) strain gage load balance (no torsion measurement) was constructed to measure the wind loads on a 1/2 scale model of a PV tile (Fig. 1). The base load balance was calibrated by applying known forces through a calibrated set of weights acting over a low-friction pulley. The various components of lift, drag, and moments were extracted from the strain-gage signals via data acquisition and reduction software. Measurements were converted to field scale values using dimensionless parameters and field scale dimensions.

A 1/2 scale model of a 10° sloped PV tile was constructed out of foam board, aluminum sheets, wood, glue and machine screws. A duplicate tile was built of Plexiglas to enhance visualization. Eight additional dummy tiles and 1/2 scale model curbs were also placed about the PV tile attached to the load balance (Figs 2 and 3). The dimensions were such that an array 3 x 3 in size could be installed in the 72 inch wide Industrial Aerodynamics Wind Tunnel, Wind Engineering and Fluids Laboratory, at Colorado State University. Visualization was performed separately in a low turbulence smooth flow environment using an argon-ion laser to create a high intensity sheet of light in the x-z plane passing through a vertical plane of the 1/2 scale PV tile model. A modified Rosco™ fog machine released visible smoke from either inside the PV tile or from a vertical line source upwind of the model. Video recordings were obtained for a variety of tile configurations.

Tunnel reference speed was approximately 10 to 11 m/s during all load tests. The tunnel ceiling was adjusted to maintain a minimal along wind static pressure gradient. A total of 92 separate run conditions were evaluated. Some of the alternative configurations included tests with no deflector present, solid deflectors with specified gaps, slotted deflectors with large and small openings, the addition of spoilers of various angles, the presence or absence of curbs, attachments added to the bottom of the PV tile to change bottom profile, deflectors with various gaps sealed with tape, deflectors raised above or below the peak of the PV tile, deflectors made of screen, addition of suction boxes and suction tubes to transfer low pressures over the peak of a PV tile to underneath it, various variations in tile gaps and spacing, and, of course, the active load tile placed in different locations within the 9 tile array (i.e.. front, middle or back row, and side or center). Measurements were also made for wind flow directed into the face of PV panel, into the face of the deflector and from the side. All test conditions were repeated multiple times. A prototype (control) test condition was selected which consisted of two rows of PV tiles, three PV tiles in each row; the center tile in the first row as on the load balance; a curb spanned the deflector sides of the front three tiles; wind blew straight toward the wind deflectors; a straight and solid deflector with a 2" top gap, and open sides.

Once effective lift, drag and moments were extracted from the measurements, the data were used to predict the “Lateral” failure wind speed,  $U_L$ , at which the 10° PV tile would start to slide given a static friction of  $\mu = 0.55$  and a tile weight at full scale of 80 pounds. Also calculated was the “Vertical” failure wind speed,  $U_V$ , at which the 10° PV tile would lift off the ground given it was restricted from lateral motion by a curb. The lateral and vertical failure wind speeds were calculated from:

$$U_L = \sqrt{\frac{\mu W}{(C_D A_D + \mu C_L A_L)(\rho/2g)}}$$

$$U_V = \sqrt{\frac{W}{(C_L A_L)(\rho/2g)}}$$

Where  $C_D$  and  $C_L$  are the non-dimensional lift and drag coefficients and  $A_D$  (height times width) and  $A_L$  (width times length) are reference areas used in the formation of the lift and drag coefficients. Lateral failure wind speed will always be less than the vertical failure wind speed for non-zero drag coefficients. Eight separate tests of the control PV distributed throughout the 90

test series revealed that standard deviations in  $C_D$ ,  $C_L$ ,  $U_L$ , and  $U_V$  were less than 4.4%, 11.4%, 2.2% and 6.3%, respectively. All measurements are tabulated in the report by Neff and Bienkiewicz (2000).

### 3 NUMERICAL MODELING PROGRAM

The CFD program Fluent<sup>®</sup> was employed to find the surface pressure distribution on both sides of the individual PV panel and its deflector. A module in the Fluent<sup>®</sup> program was used to integrate these surface pressure distributions and the opposite surfaces of the panel and deflector were subtracted to produce a net force vector acting on the panel and deflector. Summation of the downwind force vector components ( $F_x$ ) produced the mean drag. Summation of the vertical force vector components ( $F_z$ ) produced the uplift force. The overturning moment was calculated via a module within Fluent<sup>®</sup> after defining the point at which the moment should be calculated (middle of the bottom surface of the base tile). Both 2 and 3 dimensional calculations were completed using the FLUENT<sup>®</sup> CFD code with standard k-epsilon, RNG k-epsilon, or k-omega turbulent closure algorithms. Calculations were repeated until small residuals were obtained (~1000 iterations).

#### 3.1 *Two-Dimensional CFD Models*

Computations were performed for single, double, and multiple collector arrangements. For 2-dimensional situations the PV panels were inserted within a 13 m x 3 m domain that was discretized with 50,000 cells of rectangular and triangular elements distributed to produce maximum resolution along the panel surfaces. The panels were subjected to a 10 m/sec inlet profile of 15% turbulent intensity and 1 m integral scale (Fig. 4).

#### 3.2 *Three-Dimensional CFD Models*

Three dimensional computations were performed for 0° and 180° PV orientations in a 13 m x 3 m x 0.61 m domain that was discretized with 0.6 million cells of tetrahedral shape again distributed to produce finer resolution about the panels and curb. The panels were subjected to a 10 m/s inlet profile of 15% turbulent intensity and 1 m integral scale (Fig. 5).

## 4 MODEL RESULTS

Both the RNG and k-omega approaches had reasonable agreement with the measured lift and drag loads, whereas the k-epsilon approach failed to produce reduced drag at the second tile position. The k-epsilon approach also had the greatest deviations from the measured data for all three loads (drag, lift, overturning moment). The k-omega approach had the best agreement in predicting the overturning moment. Static pressure contours, velocity magnitude contours, turbulent intensity contours, vertical velocity profiles, xz plane velocity vectors near the front of the array, xz plane velocity vectors near the back of the array, xy plane velocity vectors for the 0° and 180° orientation, and particle path lines were also considered for different wind orientations. Many of the flow characteristics observed agree quite well with flow visualization observations made during the equivalent wind-tunnel tests, e.g., internal flow circulation pattern, the venting of flow out through the top gap, the separation of flow over the top, etc.

#### 4.1 *Two-Dimensional Model CFD Results*

The preliminary results generated by the 2-dimensional CFD models provided initial insight into the kinematics of flow above and around conceptual solar array arrangements. They identified the effects of curbs around the arrays, the relative influence of winds blowing from  $0^\circ$  and  $180^\circ$  orientations, and the value of the vent openings placed along the top and bottom edges of the panels. Static pressure contours for flow over the CFD 2-d model are displayed in Figure 6. From such distributions lift and drag coefficients were calculated.

The calculations of overall loads (both drag and lift) for each of the three PV tile positions are compared against the wind-tunnel measurements cited in Neff and Bienkiewicz (2000) in Figure 7. The comparison between wind-tunnel and 2-d CFD results (especially  $WD = 0^\circ$ ) in this figure suggests that the flow field over and inside PV tile arrays may be influenced by three dimensional effects. The comparison for the  $180^\circ$  wind direction is better than for the  $0^\circ$  due to the less pronounced wind penetration between the low angle PV panels versus the higher angle deflectors. The wind penetrates the gaps between adjacent deflectors and/or PV panels and the interior supports prevent uniform distribution of air flow causing strong three dimensional flow patterns.

#### 4.2 *Three-Dimensional Model CFD Results*

The static pressure contours displayed in Figure 8 are modified from their 2-d counterparts by the presence of cross-flow circulations and the blocking effects of the internal PV support structure. Inclusion of these nuances of the flow field in the calculations result in significant improvement in the numerical predictions of load.

Figure 9 presents the overall load comparisons for both the  $0^\circ$  and the  $180^\circ$  wind directions using the k-omega approach for the 3-d PV tiles. Again there is reasonable agreement for both wind directions in lift and drag and the agreement in overturning moment is quite good. The comparisons between measured data and CFD data displayed in this figure were good enough to validate the use of CFD calculations for comparative PV tile performance evaluations on other PV configurations.

## 5 SUMMARY

This paper presents the results of a hybrid numerical and physical model program to predict wind loads on photo-voltaic collector arrays. The validity of the CFD calculations were confirmed by comparisons of numerical particle tracks and smoke visualization and the similarity of predicted and measured drag, lift and moment coefficients. Once verified the CFD tool was subsequently used in a followup research program to perform rapid and cost-effective comparisons of alternate PV design configurations. The best of these configurations were subsequently examined further in a wind tunnel measurement program that determined specific wind driven paver failure which could be incorporated into a design code (Neff and Meroney, 2003).

## 6 ACKNOWLEDGMENTS:

Fiscal support for this investigation by PowerLight Corporation (now SunPower Corporation) of San Jose, CA is gratefully acknowledged.

## 7 REFERENCES:

- Barkaszi, S.F. and Dunlop, J.P., 2001, Discussion of Strategies for Mounting Photovoltaic Arrays on Rooftops, *Proceedings of Solar Forum 2001, Solar Energy: The Power to Choose*, April 21-26, Washington D.C., 6 pp.
- Healey, H.M., 2009, Florida's Winds Create Installation Problems for Solar Water Heating and Photovoltaic Modules on Buildings, *Introduction to Solar Energy*, Florida Alternative Energy Corporation, <http://www.flaenergy.com/pic2r.htm>, 2009, 2 pages.
- Lee, S. and Bienkiewicz, B., 1995, Wind Engineering Study of PowerGuard Roofing System, Technical Report for PowerLight Corporation, Wind Engineering and Fluids Laboratory, Colorado State University, Fort Collins, 192 pp.
- Neff, D.E. and Bienkiewicz, B., 2000, Wind Tunnel Study of PowerGuard RT Arrays, Technical Report for PowerLight Corporation, Wind Engineering and Fluids Laboratory, Colorado State University, Fort Collins, February, 175 pp.
- Neff, D.E. and Meroney, R.N., 2003, *Wind Performance of Photovoltaic Arrays*, Final Report, Wind Engineering and Fluids Laboratory, Colorado State University, 181 pp
- O'Brien, C., 2006, Roof-mounted Solar Photovoltaic Arrays: Technical Issues for the Roofing Industry, *Interface, Trade Journal of RCI, Inc.*, March, pp. 13-22.
- Radu, A., Axinte, E., and Theohari, C., 1986, Steady Wind Pressures on Solar Collectors on Flat-Roofed Buildings, *J. Wind Engr. Ind. Aero.*, Vol. 23, pp. 249-258.

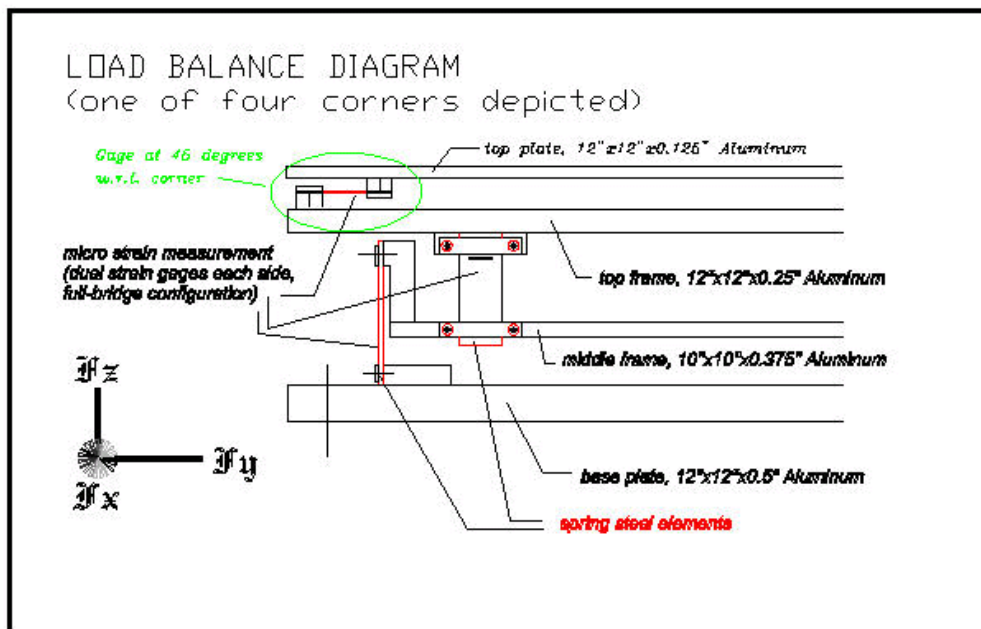


Figure 1. Load Measurement Balance

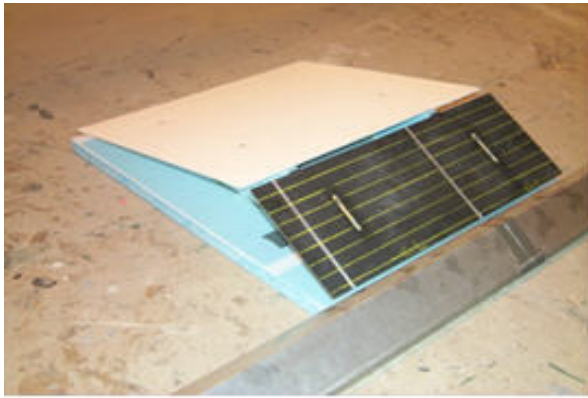


Figure 2. 1/2 Scale load testing PV control tile, 10° slope and curb.

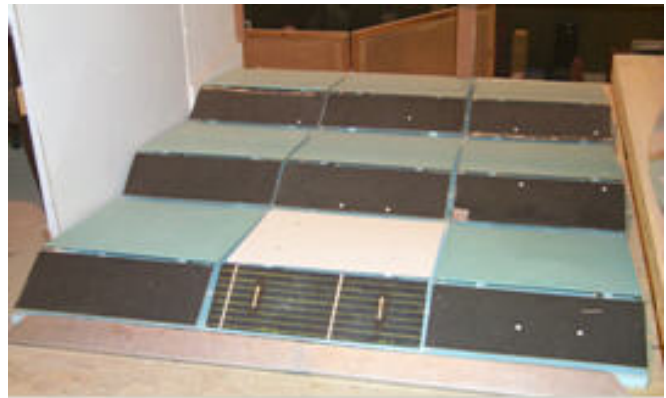


Figure 3. 1/2 Scale control tile combined with 8 dummy tiles and curb.

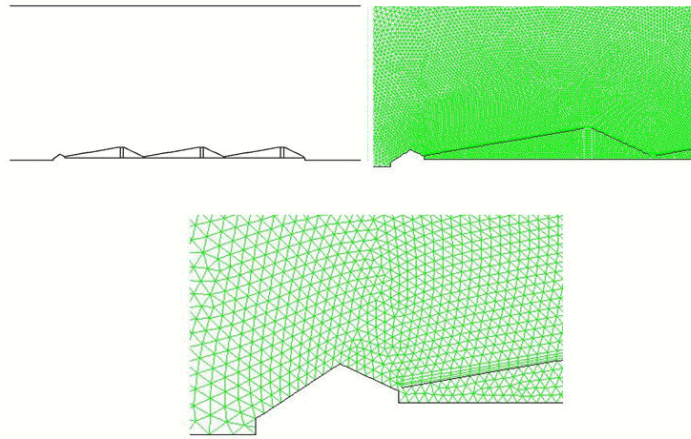


Figure 4. CFD 2-d Model and Grid Layout

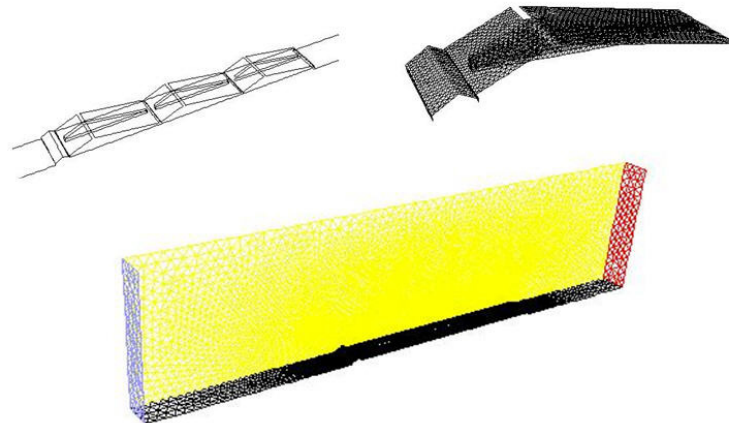


Figure 5. CFD 3-d Model and Grid Layout

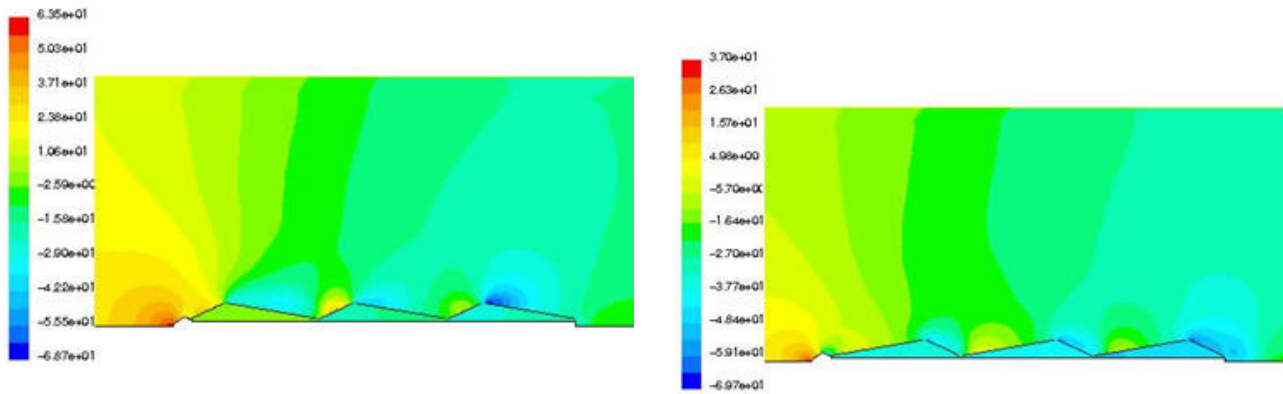


Figure 6. Static Pressure Contours for CFD 2-d Model (left - 0° and right 180° wind orientations).

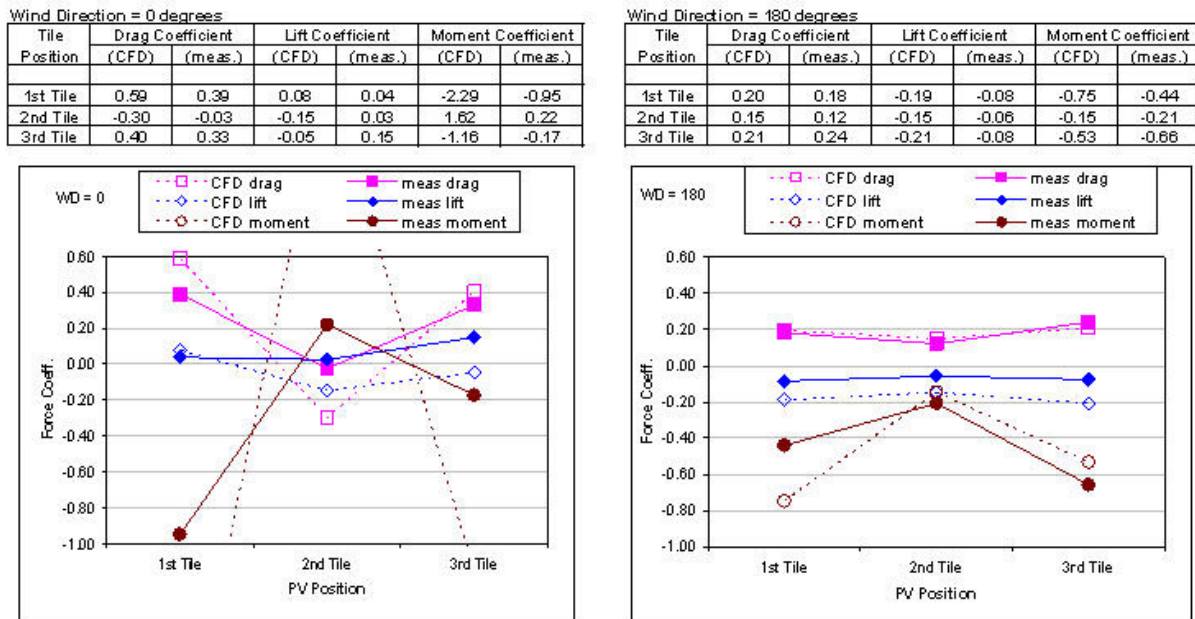


Figure 7. Overall Load Comparisons between CFD 2-d and Wind-Tunnel Tests

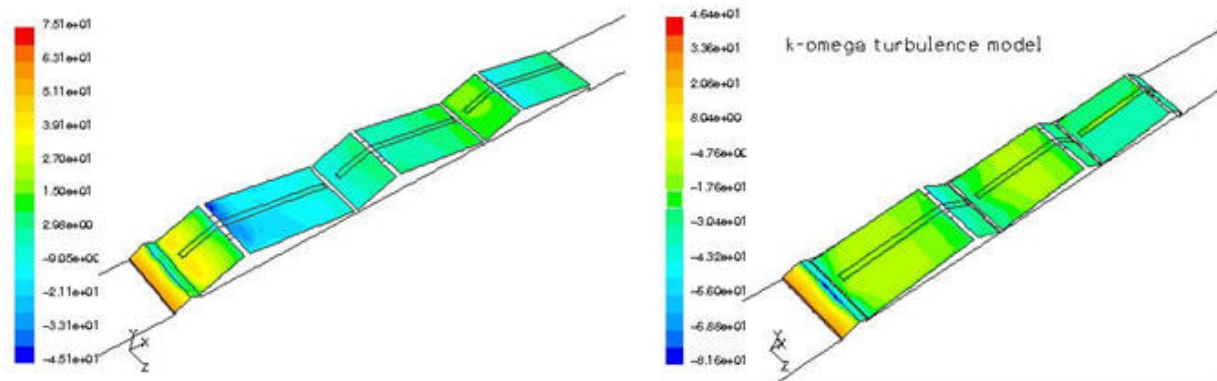


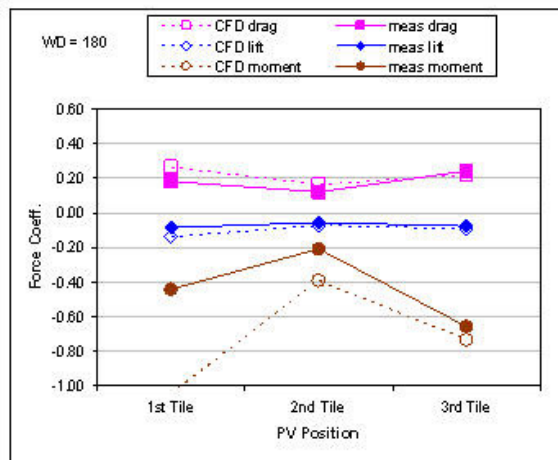
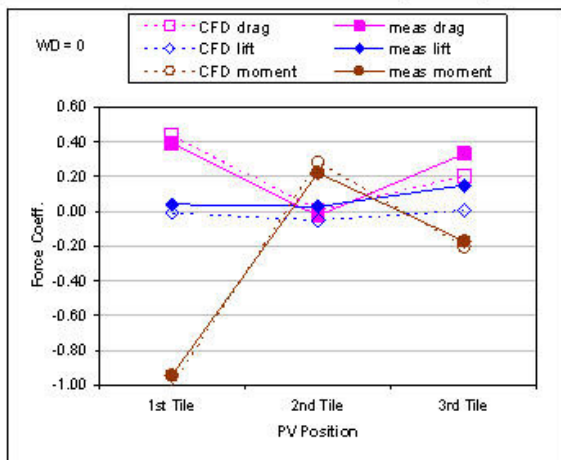
Figure 8 Static Pressure Contours for CFD 3-d Model (left - 0° and right 180° wind orientations).

Wind Direction = 0 degrees (towards deflector)

Tile Position	Drag Coefficient		Lift Coefficient		Moment Coefficient	
	(CFD)	(meas.)	(CFD)	(meas.)	(CFD)	(meas.)
1st Tile	0.43	0.39	-0.01	0.04	-1.00	-0.95
2nd Tile	0.01	-0.03	-0.05	0.03	0.28	0.22
3rd Tile	0.20	0.33	0.00	0.15	-0.20	-0.17

Wind Direction = 180 degrees (towards PV)

Tile Position	Drag Coefficient		Lift Coefficient		Moment Coefficient	
	(CFD)	(meas.)	(CFD)	(meas.)	(CFD)	(meas.)
1st Tile	0.27	0.18	-0.14	-0.08	-1.04	-0.44
2nd Tile	0.16	0.12	-0.07	-0.06	-0.39	-0.21
3rd Tile	0.22	0.24	-0.09	-0.08	-0.73	-0.66



Ref. Velocity for coefficients was at Boundary Layer Height.

Figure 9 Overall Load Comparisons between CFD 3D and Wind-Tunnel Models